DEMONSTRATION OF THE IFM NANO FEEP THRUSTER IN LOW EARTH ORBIT

David Krejci [(1)], Alexander Reissner [(1)], Bernhard Seifert [(2)], David Jelem [(2)], Thomas Hörbe [(2)], Florin Plesescu[(2)], Pete Friedhoff [(3)], Steve Lai [(3)]

[(1)]ENPULSION, Viktor Kaplan-Strasse 5, Wiener Neustadt, 2700, Austria, krejci@enpulsion.com
[(2)]FOTEC, Viktor Kaplan-Strasse 5, Wiener Neustadt, 2700, Austria, seifet@fotec.at
[(3)]Planet, 1245 Terra Bella, Mountain View, 94043, CA, friedhoff@planet.com

ABSTRACT

The IFM Nano Thruster is a variable specific impulse electrostatic thruster based on Field Emission Electric Propulsion (FEEP), in which a liquid propellant is electrostatically extracted and accelerated to high exhaust velocity. The core element of this propulsion technology is a passively fed, porous ion emitter consisting of 28 sharp emitter tips. This emitter technology has been developed and qualified over decades at FOTEC and the Austrian Institute of Technology, and has recently been adapted for the use as main propulsion system in Nano- and Small-satellites. The resulting IFM Nano Thruster occupies approximately 0.8 U and can be operated between 10 and 40W, resulting in thrust of up to 0.35mN. The thruster can be operated at specific impulse levels between 2000s and 6000s, adapting to mission needs as well as power availability, allowing for significant throttling capability between a couple of µN and 0.5mN. Due to the high specific impulse and high propellant density, the thruster can produce total impulses between 5000Ns and beyond 12000Ns when operated at specific impulses at 2000s and 5000s respectively. The first IFM Nano Thruster has been successfully integrated into a commercial 3U CubeSat in 2017 after undergoing environmental testing, and was launched in January 2018 for a first in-orbit demonstration (IOD). This IOD represents the first instance of a liquid metal FEEP thruster to be operated in space as a primary propulsion system. This paper will present the FEEP thruster principle and experimental characterization, including the first in-orbit test results.

1 INTRODUCTION

Small, compact propulsion is considered an enabling technology for high performing Nano- and Smallsat missions, including scientific missions and formation flying missions [1],[2],[3]. In addition, propulsive capabilities can be used for life extension in LEO orbits and high total impulse propulsion can enable interplanetary missions [4]. Scalability of satellite and propulsion technologies allows for large constellation architectures for a variety of applications, including high temporal resolution earth observation and telecommunication network applications. One of the technologies investigated to fill the current need for compact, high performing propulsion is liquid metal FEEP propulsion [5], [6],[7], which allows for high specific impulse due to the electrostatic acceleration principle [8] and high total impulse due to the high density of the propellant. Liquid metal indium sources have been developed for over 25 years at the FOTEC (former Austrian Institute of Technology) and have gained considerable space heritage [9]. Based on this technology, liquid metal FEEP emitters for propulsive applications have been developed and extensively tested, resulting in a multi-emitter design shown in Fig. 2 during emission.

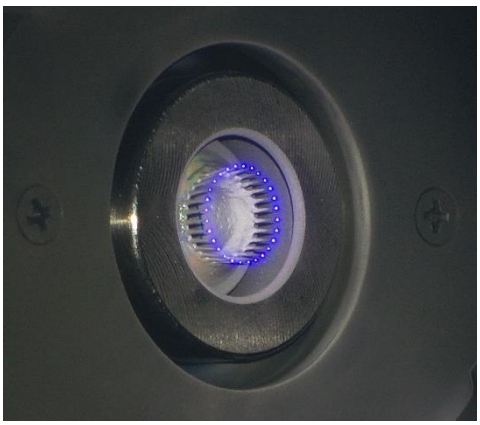

Figure 2. Closeup of IFM Nano Thruster during ion emission

2 THE IFM NANO THRUSTER

2.1 Operating Principle

Field Emission Electric Propulsion is based on extraction and ionization of propellant from a liquid metal, a process that can occur at field strengths in the order of 1Vnm^{-1}. To achieve the necessary local field strength, the liquid metal is usually suspended over a sharp emitter structure in needle form. Different configurations for passive propellant transport by capillary forces have been investigated, including capillary geometries, externally wetted needles and porous needle-like structures. Electrostatic stressing of the liquid metal above a certain threshold causes the metal to deform into a Taylor cone [10], further increasing the local field strength at the apex of the cone, where particle extraction is eventually achieved. In a FEEP device, the electrostatic potential is applied between the metal emitter and a counter electrode called extractor, which is designed to maximize transparency for emitted ions. In such a geometry, ions are then accelerated by the same electric field used for extraction and ionization, making this process highly efficient. In addition to ions, instabilities in the Taylor cone and the jet [11],[12] lead to additional expulsion of droplets, which do not contribute to the thrust, but lead to a net increase in the average propellant mass flow, therefore decreasing the specific impulse achieved [14]. The thrust F and specific impulse I_{sp} of a FEEP thruster can be approximated by Eq. 1 and Eq. 2 respectively [15]

$$F = I \cdot \sqrt{2 \cdot V_e \cdot \frac{m}{q_e}} \cdot f \tag{1}$$

$$I_{sp} = \frac{1}{g_0} \cdot \sqrt{2 \cdot V_e \cdot \frac{q_e}{m}} \cdot \eta \cdot f \tag{2}$$

in which I is the net emitted current, V_e is the emitter potential, q_e/m is the mass-to-charge ratio of a singly ionized indium ion and g_0 is the standard acceleration due to gravity. f is a factor accounting for the beam spreading and according radial component of particle velocity which does not contribute to thrust and η is the mass efficiency of the emitter, which is a function of the emission current and emitter properties, and can be characterize for each emitter during acceptance testing.

Since a FEEP emitter expels positively charged ions, with electrons tunneling back into the metal propellant and therefore remaining within the thruster system, an additional means for electron emission is necessary to avoid charging of the thruster, and hence the entire spacecraft. A variety of

different electron emitters are available, including thermionic neutralizers and electron emitters based on carbon nanotube forests [16].

2.2 The IFM Nano Thruster

Figure 1. IFM Nano Thruster

The IFM Nano Thruster shown in Figure 1 is a compact packaging of the heritage ion emitter, propellant reservoir, neutralizer and power processing unit in a Cubesat sized form factor with approximately 80mm height. It has been developed at FOTEC and is now introduced to the commercial market by ENPULSION. The thruster utilizes a metal propellant that is in solidified stated during ground handling and launch. The IFM Nano Thruster features two neutralizers in cold redundancy, and a digital PPU which provides power and control for all necessary subsections to operate the thruster, and provides telemetry back to the spacecraft onboard computer using either RS422 or RS485 interface. By controlling voltages of both the emitter and the extractor, the emission current, and thus the resulting thrust, can be decoupled from the acceleration potential, and hence the specific impulse. This allows to operate the thruster in an envelope of specific impulse and thrust. Figure 2 shows the operational envelope of an IFM Nano Thruster with 35% mass efficiency (at 4mA emission current), plotting thrust and specific impulse as a function of total system input power. This total input power includes the beam power with corresponding efficiencies, the power necessary for housekeeping, the heater to maintain the propellant in liquid state and the neutralizer. In the current version of the IFM Nano Thruster, the PPU is designed for a maximum input power of up to 40W. The iso-power lines in Figure 2 indicate the operational points available for a given input power. In a spacecraft with 40W available for propulsion, the IFM Nano Thruster depicted can, for example, be operated at a thrust of F~0.42mN with specific impulse of 3200s for a maneuver where higher thrust is required, consuming a total input power of 40W, and could then be used in another stage of the mission at F~0.25mN and an I_{sp} of 5000s at a reduced input power of ~30W in a mission stage lower thrust levels but high specific impulse are desired.

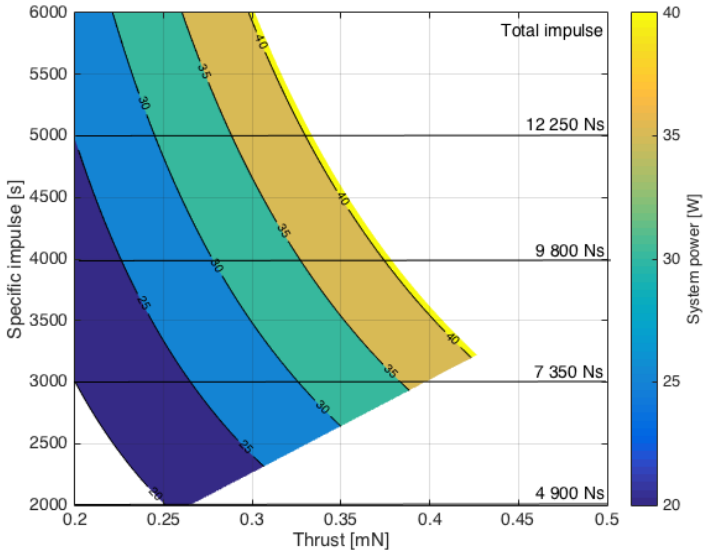

Figure 2. Performance envelope of the IFM Nano Thruster

3 IN-ORBIT DEMONSTRATION

3.1 Satellite description and early commissioning phase

One IFM Nano Thruster was integrated in a 3U Cubesat in 2017, and launched into a 491 x 510 km orbit on January 12, 2018 on PSLV-C40. The spacecraft is equipped with reaction wheels for attitude control, which are also used to counteract eventual thrust vector offset.

Before thrust operation was attempted, the functionality of the different subsections of the thruster was verified in a detailed commissioning phase, described in [17]. This included proper readout of onboard telemetry including temperature measurements, and functional verification of the heater, emitter and extractor voltage supplies and neutralizer section. After verification of full functionality of the individual sections, thrusting capability of the IFM Nano Thruster was verified.

3.2 Propellant liquification

The IFM Nano Thruster requires liquification of the propellant, which then needs to be controlled to the operational temperature throughout the changing thermal environment during orbital cycles. In the test shown in Figure 3, initial heating was performed using a constant set power of 8W, followed by a fully automatic control with a 10W limit. The heater was briefly switched off when changing from constant power to automatic control, as can be clearly seen around 28min relative time. Approximately 1h 20mins into the test, the phase change of the propellant started to occur, lasting for approximately 20mins, which is clearly distinguishable in the temperature plateau until full liquification is achieved and the propellant temperature rises again. After achieving the operational temperature at 1h 51min into the test, the controller decreased the heater power to maintain the operational temperature, and was able to maintain temperature during the eclipse pass of the spacecraft. During this time period, the IFM Nano Thruster is in a ‘hot standby’ state, meaning that thrust could be commanded instantly.

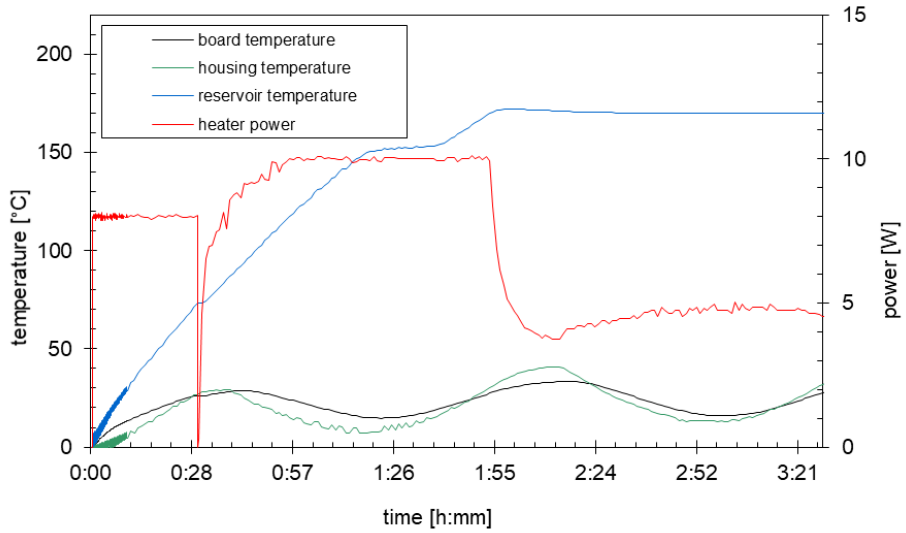

Figure 3. In-orbit verification: Propellant liquification and maintaining operational temperature throughout eclipse

The telemetry data shown in Figure 3 verifies the functionality of the heater section to liquify the propellant and perform stable control of the propellant temperature at the commanded operational temperature, with minimal increase in housing and board temperature.

Comparison of the data to the theoretical melting temperature of Indium allows to determine an offset of the measurement of only 5°C of the ground calibration performed before thruster integration, and allows to recalibrate the temperature measurement in-orbit for subsequent tests.

3.3 Neutralizer operation

To prevent charging of the spacecraft during ion emission, a neutralizer is used to emit electrons, at a bias voltage of -220V. Overcompensation guarantees maximum spacecraft potential shift to +220V, avoiding drift to the kV range of the emitter. Before liquid metal ion emission was attempted, the functionality of the neutralizer was verified in a test sequence where only the neutralizer was operated. This test sequence consisted of commanding a linearly increasing ramp of the electron emission current from zero to 5mA, which is 125% of the maximum ion emission current in the IFM Nano Thruster, and a corresponding ramp back to zero.

Figure 4 shows the telemetry gathered during this neutralizer functionality test. At 55s into the test, the bias voltage is commanded to -220V, and the commanded current ramp is subsequently started at 1min into the test. It can be seen that in the initial heat-up of the filament, the measured emission current initially lags the commanded current profile until the emission filament is brought up to the working temperature at approximately 1m 26s. After this, expected, onset behavior, the electron emission current is closely following the commanded current profile, within the limited resolution available for the electron emission current measurement. In addition to the emission current, Figure 4 plots the duty cycle of the neutralizer supply, which reproduced the behavior expected from ground testing.

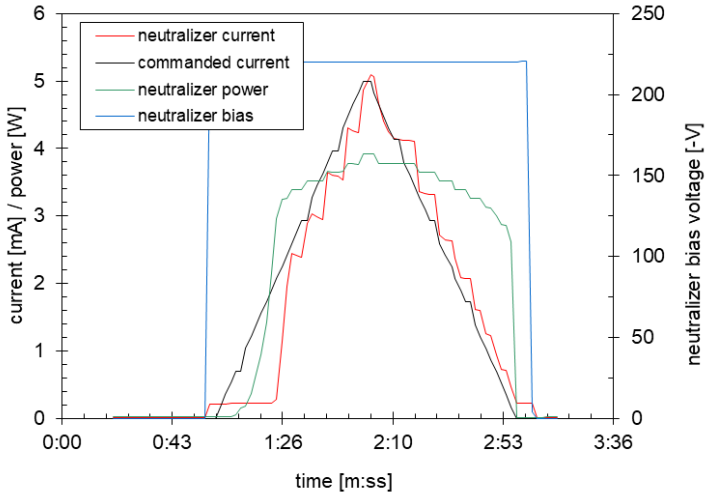

Figure 4. In-orbit verification: Functional test of the neutralizer

3.4 Thrusting operation

After successful verification of the functionality of all subsections of the IFM Nano Thruster, commissioning tests of the ion emitter have been performed [17]. These test sequences included propellant liquification, operation of the neutralizer, and ion emission. After neutralizer emission had been established, the emitter current was commanded a linear ramp from zero to 2mA. Figure 5 shows the emission current response, as well as the emitter potential necessary to achieve the commanded emission current. In addition, the current measured in the extractor, that is charged particles impacting the extractor after emission, is plotted.

The data in Figure 5 shows the immediate onset of emission current, which then closely follows the commanded current profile. The current intercepted in the extractor is found less than 0.2%.

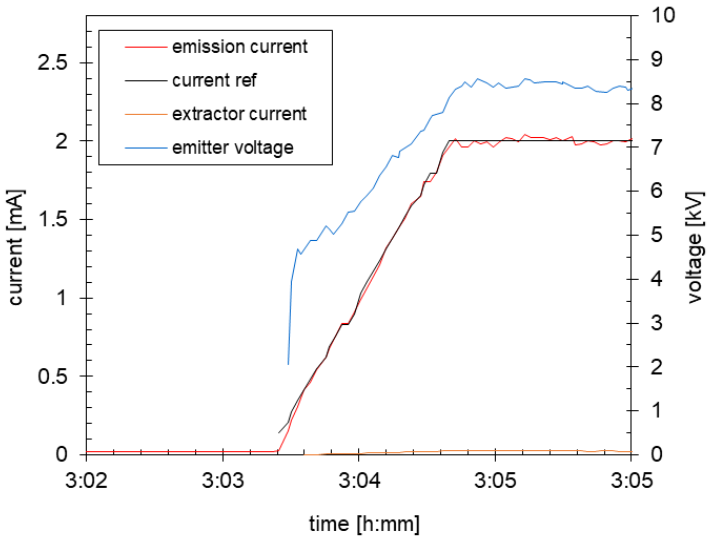

Figure 5. In-orbit verification: Start-up of the emitter during commanded current ramp

3.5 Independent thrust verification test

3.5.1 Test 1: 15-minute firing

A burn of 15 minutes duration at 2mA emission current was conducted to allow for independent verification of the thrust produced by the IFM Nano Thruster. Before thrust activation, the spacecraft was aligned using reaction wheels, in a way that the thruster was oriented along the velocity vector to increase the spacecraft orbital velocity, and attitude was maintained with the help of the reaction wheels throughout the firing period. The test was again started from cold state, with constant heating power for the initial 30mins of the test, followed by automatic heater control. Figure 6 shows the temperature profiles during the test, showing the increase in reservoir temperature up to the enthalpy step, followed by subsequent increase to the operating temperature, and control to this temperature throughout changing thermal environment. The temperature of the PPU PCB as well as the thruster housing are plotted in addition, showing the expected thermal cycle behavior due to orbital cycling. After 3hours and 3minutes into the test, thrust was commanded, which lead to an increase of the PPU board temperature due to dissipated power in the electronics. Based on the data available, the temperature increase is expected to level off at approximately 70°C, which is still in bounds of the operational temperature of the PPU. In addition, the thrusting maneuver was commanded after the spacecraft exited eclipse, and the increase in board temperature due to power dissipation is therefore superimposed by the increase due to change in thermal environment.

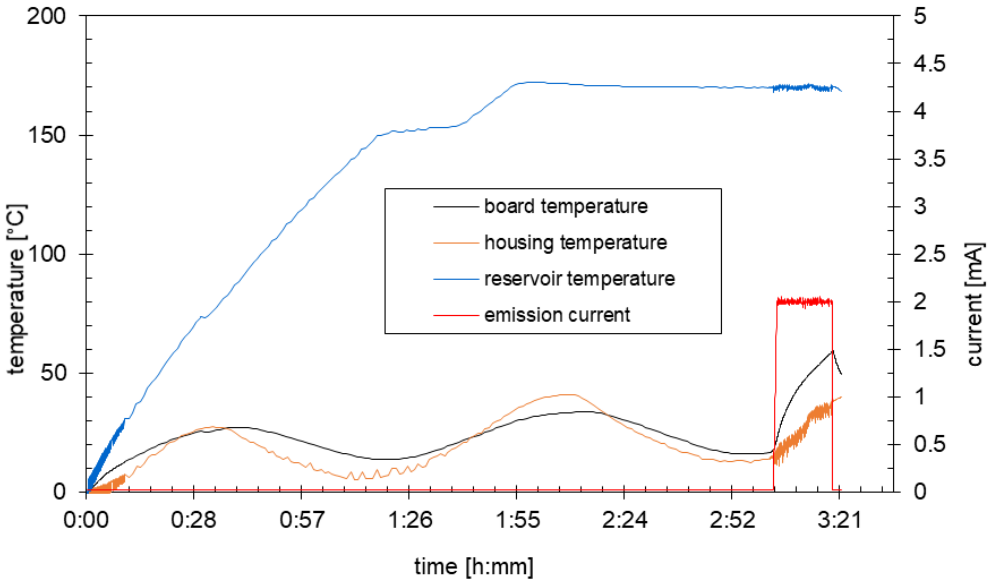

Figure 6. In-orbit verification: Temperature of propellant and thruster components during entire test, 15 min firing period distinguishable by emission current measurement

Figure 7 shows a detail of the thrusting phase of this test, plotting the commanded emission current, the measured emission current, the emitter voltage and the extractor current. In this test, the emission voltage of the thruster was commanded to increase linearly from zero to 2mA within 60s, followed by 15min of firing at 2mA. In this test, the emitter was operated in a current controlled mode.

The telemetry shown in Figure 7 verifies the ability of the thruster to closely follow the commanded current ramp, as well as to maintain the constant current level. The emitter voltage to achieve the commanded current, in addition to a constantly biased extractor, is plotted and shows, after initial

increase during the current ramp, a slight decrease, indicating a decreasing emitter impedance, which is expected during the initial firing phases of a FEEP emitter [18].

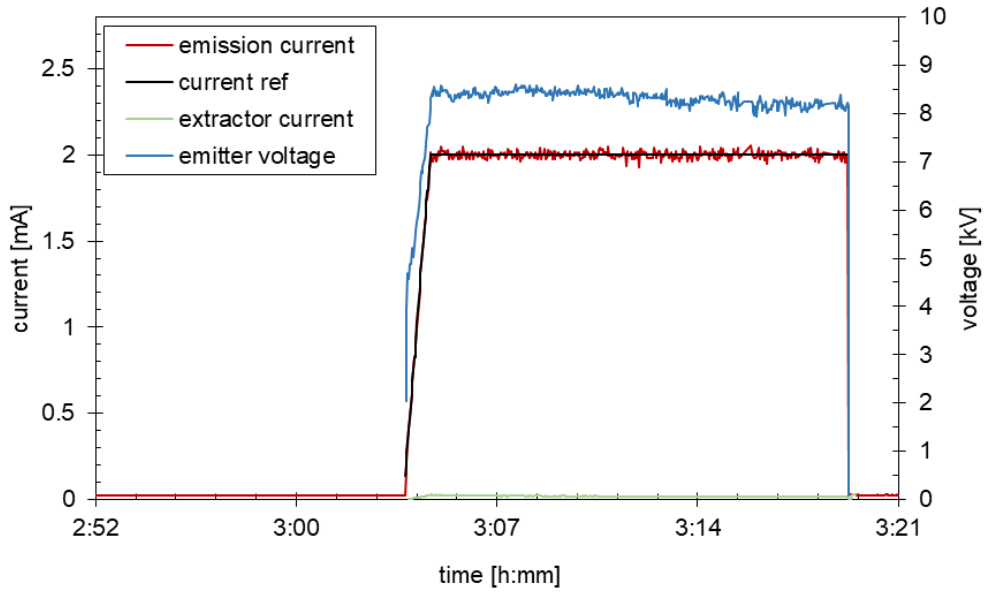

Figure 7. In-orbit verification: Commanded emission mission current (black) versus measured emission current (red) during 15 min firing

Using existing models for the mass efficiency of the 28-needle emitter crown [19], the thrust and specific impulse are calculated by the IFM Nano Thruster according to Eq. 1 and 2 respectively. This data is shown in Figure 8, where a mass efficiency of 40% is assumed for an emission current of 2mA. Operating in current control mode at 2mA emission current resulted in a thrust of F = 0.2232 ± 0.0026 mN average over the 15-minute firing period.

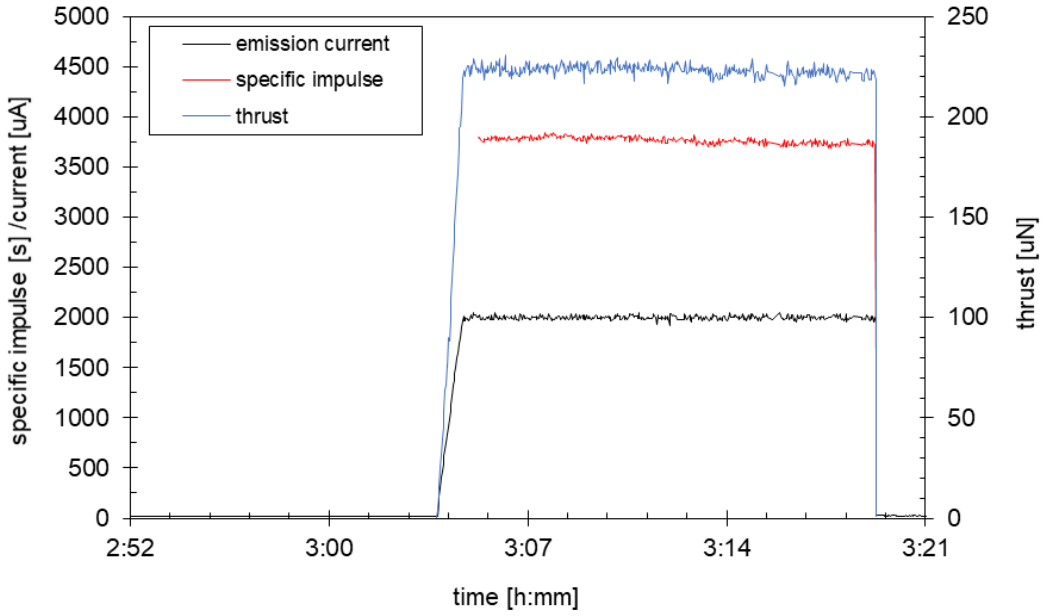

Figure 8. In-orbit verification: Calculated thrust and estimated specific impulse during 15 min firing

3.5.2 Test 2: 30-minute firing

In a subsequent test, a 30-minute burn was conducted, again with emission current controlled in a ramp to 2mA, followed by 30 minutes at 2mA. Figure 9 shows the commanded and measured emission current, emitter voltage, as well as resulting thrust and specific impulse during the firing maneuver.

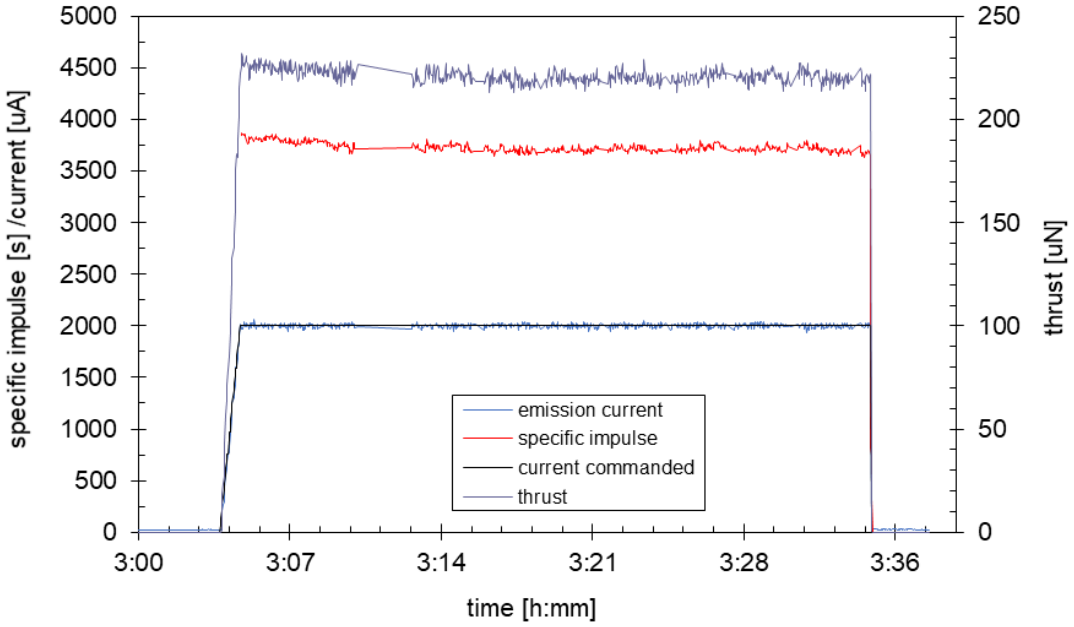

Figure 9. In-orbit verification: Telemetry data for 30 min firing.

Figure 9 plots a detail of the telemetry data during the firing phase of the test. If clearly shows the thrusters ability to closely follow the commanded current ramp, and plots the corresponding thrust and specific impulse values, showing again stable operation.

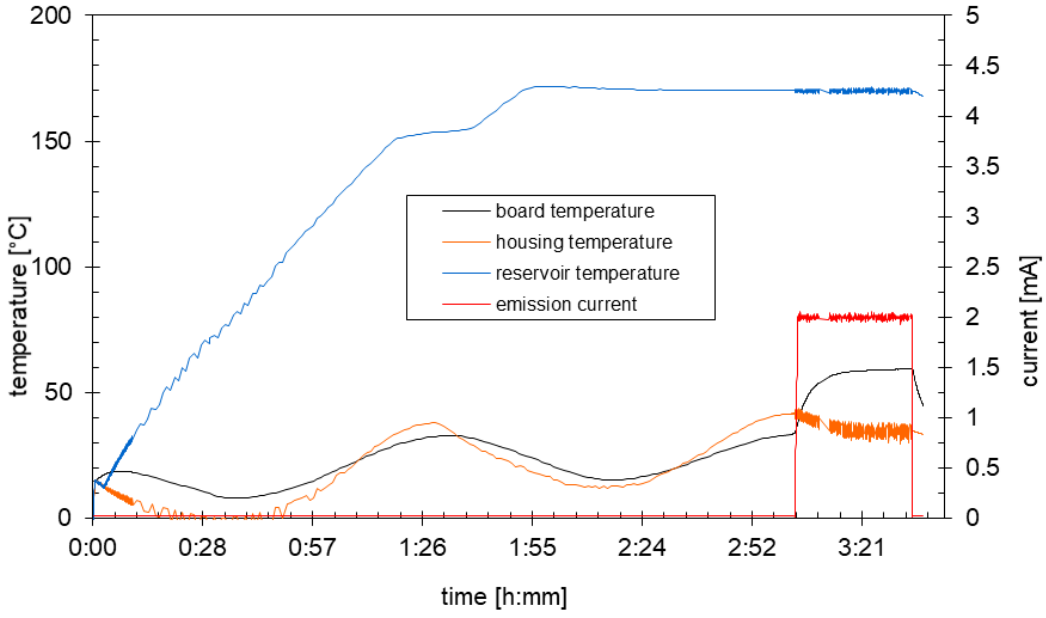

Figure 10. In-orbit verification: Temperature profiles for 30 min firing.

During this test, the attitude of the satellite was not maintained parts of the firing duration, decreasing the effective thrust along the spacecraft velocity vector to 82% of the total thrust force, leading to an effective change in velocity of 6.6cm/s. Operating in current control mode at 2mA emission current, the average thrust determined by thruster telemetry was $F = 0.2212 \pm 0.0033$ mN average over the 30 minute firing period, with an estimated specific impulse of approximately 3650-3750s.

The test was scheduled in a way that thrusting operation would occur during eclipse, validating the satellites ability to fire the thruster during this orbital phase. Figure 10 shows the temperature telemetry during the entire test including propellant liquefication. During the firing phase, the rapid increase in board temperature is noticeable, with PPU temperature levelling off below 60°C, which is well inside the operational range of the IFM Nano Thruster PPU.

3.5.3 Independent orbit change verification

Before and after the thrust maneuver, GPS data was collected for precise determination of the orbit before and after burn. Analysis of the different error contributions lead to estimating the maximum pointing inaccuracy of the spacecraft during the thrust operation to be within 10deg. The GPS data was then processed using a 50x50 gravity model. Based on the telemetry provided by the thruster, and spacecraft properties and expected alignment, the expected orbit altitude change for the 15-minute maneuver was calculated as 72m. Comparison of orbit determination before and after the thrust maneuver showed an average orbit height difference of 70 ± 5m. In case of the 30-minute maneuver, the height change based on telemetry data and satellite attitude was calculated as 115m, with GPS data taken before and after the maneuver showing an average orbital height difference of 116m. The comparison of orbit changes calculated based on thruster telemetry data and measured using GPS is summarized in Table 1.

Table 1. Change in average spacecraft semi-major axis due to thrust maneuver, measured from GPS data and calculated from propulsion telemetry

Maneuver parameters	**Average change in semi-major axis [m]**	
	Calculated from thruster telemetry	GPS measurements
Test 1: I_{em}=2mA, 15 min	72	70 ± 5
Test 2: I_{em}=2mA, 30 min	115	116 ± 5

4 CONCLUSION

The IFM Nano Thruster, a Cubesat sized liquid metal FEEP thruster has been tested on board of a 3U Cubesat. After an extensive commissioning phase, in which the functionality of all subsections of the thruster was verified, first thrust maneuvers have been performed. After initial short firing tests, a first constant thrust maneuver with 15 minutes duration has been performed, with the spacecraft ADCS maintaining thrust vector alignment. Comparison of GPS data before and after the thrust maneuver verified an average semi-major axis change of the spacecraft by 70 ± 5m. This change in orbital altitude corresponds very well with the expected 72m height change that was expected based on onboard telemetry provided by the thruster. This test was followed by several thrust maneuvers including a 30-minute thrusting phase, showing again good accordance between orbit change calculated from thruster telemetry and GPS measurements amounting to approximately 115m change in average orbit altitude. Throughout all ion emission phases, the spacecraft charge build-up was prevented using the thruster's neutralizer.

5 REFERENCES

[1] Krejci, D. and Lozano, P., *Space Propulsion Technology for Small Spacecraft*, Proceedings of the IEEE, Vol. 106, Iss. 3, 2018.

[2] Lemmer, K., *Propulsion for Cubesats*, Acta Astronautica, Vol. 134, 2017, pp. 231-243.

[3] Selva, D. and Krejci, D., *A Survey and Assessment of the Capabilities of Cubesats for Earth Observation*, Acta Astronautica, Vol. 74, 2012, pp. 50-68.

[4] Spangelo, S. and Longmier, B., *Optimization of CubeSat System-Level Design and Propulsion Systems for Earth-Escape Missions*, Journal of Spacecraft and Rockets, Vol. 52, No. 4, 2015, pp. 1009-1020.

[5] Vasiljevic, I., et al., *Consolidation of milli-Newton FEEP Thruster Technology based on Porous Tungsten Multiemitters*, AIAA 2011-5592, 47th AIAA/SAE/ASEE Joint Propulsion Conference, San Diego, CA, 2011.

[6] Jelem, D., et al., *Performance Mapping and Qualification of the IFM Nano Thruster FM for in Orbit Demonstration,* 53rd AIAA/SAE/ASEE Joint Propulsion Conference, Atlanta, GA, 2017.

[7] Jelem, D., et al., *Performance Mapping and Qualification of the IFM Nano Thruster FM for in Orbit Demonstration,* 35th International Electric Propulsion Conference, Atlanta, GA, 2017.

[8] Tajmar, M., et al., *Indium Field Emission Electric Propulsion Microthruster Experimental Characterization,* Journal of Propulsion and Power, Vol. 20, No. 2 2004, pp. 211-218.

[9] Fehringer, M., et al., *Space-proven indium liquid metal field ion emitters for ion microthruster applications,* 33rd Joint Propulsion Conference and Exhibit, 1997.

[10] Taylor, G. I., *Disintegration of Water Drops in an Electric Field,* Proceedings of the Royal Society A, Vol. 280, 1964, pp. 383-397.

[11] Mair, G. L. R., *Electrohydrodynamic instabilities and the energy spread of ions drawn from liquid metals,* J. Phys. D.: Appl. Phys, Vol. 29, 1996, pp. 2186-2192.

[12] Tajmar, M., *Influence of Taylor cone size on droplet generation in an indium liquid metal ion source*, Applied Physics A, Vol. 81, 2005, pp. 1447-1450.

[13] Tajmar, M., *Experimental validation of a mass-efficiency model for an indium liquid-metal ion source*, Applied Physics A, Vol. 76, 2003, pp. 1003-1006.

[14] Tajmar, M., *Experimental evaluation of the critical current in indium LMIS,* Journal of Physics D: Applied Physics, Vol. 42, 2009, 055506(4pp).

[15] Vasiljevich, I., et al., *Development of an Indium mN-FEEP Thruster,* AIAA 2008-4534, 44th AIAA/SAE/ASEE Joint Propulsion Conference, Hartford, CT, 2008.

[16] Tajmar, M., *Survey of FEEP Neutralizer Options,* AIAA 2002-4243, 38th AIAA/SAE/ASEE Joint Propulsion Conference, Indianapolis, IN, 2002.

[17] Seifert, B., et al., *In-Orbit Demonstration of the Indium-FEEP IFM Nano Thruster,,* 6th Space Propulsion Conference, Seville, Spain, 2018.

[18] Reissner, A., et al., *Testing and Modelling of the mN-FEEP Start-Up Performance,* IEPC-2015-123, 34th International Electric Propulsion Conference, Hyogo-Kobe, Japan, 2015.

[19] Vasiljevich, I., *Design, Development and testing of a highly integrated and up-scalable FEEP-multi-emitter using Indium as Propellant,* 2010.